Optimizing Energy Consumption in Hydrogen Reduction of Iron Ore Pellet: Insights from HSC Chemistry Analysis

A. Heidari, T. Fabritius

Process Metallurgy Research Unit, University of Oulu, Oulu, Finland (e-mail: aidin.heidari@oulu.fi, timo.fabritius@oulu.fi.

Abstract: Iron ore pellet reduction in shaft furnaces represents a critical process in the steelmaking industry, with energy consumption being a key factor influencing both economic viability and environmental sustainability. This study employs HSC Chemistry software to model and simulate the energy consumption of hydrogen reduction of iron ore pellets under varying water vapor content within the shaft furnace. Thermodynamic modeling was carried out as the first step to analyze the effect of water vapor on the thermodynamic equilibrium, determining the possible range of water vapor content. Subsequently, energy consumption of the process was modeled based on heat and mass balance. Through comprehensive analysis, we investigate the impact of water vapor on the overall energy efficiency of the process based on the two scenarios of supplying the required heat by preheating the feed materials or injection of oxygen to the furnace. Our findings reveal significant insights into optimizing energy consumption and operational parameters to enhance the sustainability and cost-effectiveness of iron ore pellet reduction. This research contributes to the ongoing efforts towards achieving greater efficiency and reduced environmental footprint in the steelmaking industry.

Keywords: Hydrogen Reduction of Iron ore pellets, Shaft furnace, Energy consumption, HSC Chemistry analysis

1. INTRODUCTION

Currently, more than 70% of the world's iron production is derived from the integrated blast furnace (BF) and basic oxygen furnace (BOF) process, which emits around 1.9 tons of CO_2 per ton of crude steel, as coke is the primary reducing agent. Consequently, the iron and steel industries account for about 7% of global CO_2 emissions. Using hydrogen as a reducing agent presents a solution to reduce CO_2 emissions, replacing CO_2 with H_2O as a by-product(Özgün et al., 2023; Souza Filho et al., 2023; Spreitzer and Schenk, 2019).

Hydrogen can be employed in ironmaking through three methods: hydrogen injection in blast furnaces, hydrogen direct reduction, and hydrogen plasma reduction(Ahmed et al., 2020; Raabe et al., 2023; Souza Filho et al., 2022, 2021,). Among these, hydrogen direct reduction is closest to industrialization, with several companies initiating the construction of their first hydrogen direct reduction plants(Sun et al., 2023). The schematic of process is shown in Fig. 1.

The thermodynamics and kinetics of hydrogen reduction of iron ores have been extensively studied(Fradet et al., 2023; Heidari et al., 2021). Unlike carbon monoxide reduction, hydrogen reduction is entirely endothermic, making increased temperatures thermodynamically favorable but requiring additional energy input. Hydrogen reduction is faster than carbon monoxide reduction due to hydrogen's smaller molecule size, and higher mobility and diffusivity. However, many factors, including feed characteristics (such as ore type, mineralogy, and porosity) and system parameters (such as reduction temperature, gas flow rate, and pressure), influence the process kinetics(Spreitzer and Schenk, 2019).

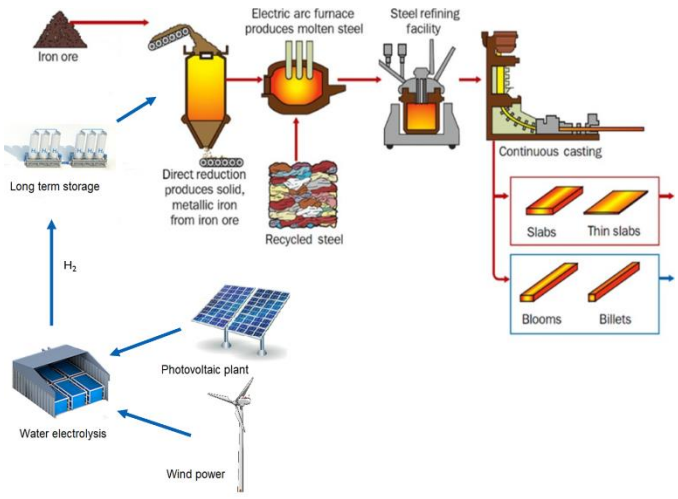

Fig. 1. The schematic of hydrogen-based fossil-free iron and steel making.

Water vapor in the shaft furnace also affects the thermodynamics, kinetics, and energy consumption of the process(El-Zoka et al., 2023). Water vapor can originate from various sources, including as a by-product of reduction reactions, moisture in the pellets from the pelletizing process, and oxygen injection for energy supply, which reacts with hydrogen to produce water vapor. Moreover, hydrogen can be produced through methods like steam methane reforming,

electrolysis of water, and natural gas pyrolysis, all of which may introduce water vapor as an impurity.

Given the presence of water vapor in the shaft furnace, it is essential to study its effects on the process from multiple perspectives. This study examines the energy consumption of the hydrogen reduction process in a shaft furnace with varying water vapor content using HSC Chemistry software.

2. HEAT AND MASS BALANCE MODEL

Hydrogen is currently utilized as a reducing agent in certain direct reduction processes like MIDREX and HYL, where hydrogen and carbon monoxide are produced by natural gas cracking in the reformer before being introduced to the shaft furnace. However, no shaft furnace operates with 100% hydrogen for real data application in our model. Thus, this study uses MIDREX process data, the leading direct reduction technology, and adapts it for the hydrogen reduction process.

In this static model, system components are divided into gas and solid phases. The gas phase includes reducing gas and top gas, while the solid phase consists of feed material and produced sponge iron (DRI). The chemical compositions of these phases are detailed in Table 1.

Table 1. Phases and chemical components considered in shaft furnace.

Phases	Chemical composition
Gas	H_2, H_2O, O_2
Solid	Fe_2O_3, Fe_3O_4, Fe, SiO_2, CaO, MgO, Al_2O_3, TiO_2, MnO

Hydrogen reduction process includes three stages of reduction of hematite to magnetite, magnetite to wüstite, and wüstite to metallic iron as it is presented by the reactions 1, 2, and 3 respectively.

$$3\,Fe_2O_3\,(s) + H_2\,(g) = 2\,Fe_3O_4\,(s) + H_2O\,(g) \quad (1)$$

$$Fe_3O_4\,(s) + H_2\,(g) = 3\,FeO\,(s) + H_2O\,(g) \quad (2)$$

$$FeO\,(s) + H_2\,(g) = Fe\,(s) + H_2O\,(g) \quad (3)$$

Moreover, oxygen can be introduced to the shaft furnace and the combustion of hydrogen takes place through the reaction 4 to supply the required heat of reduction reactions.

$$H_2 + \frac{1}{2}O_2 = H_2O \quad (4)$$

2.1 Mass balance

The mas balance model that has been used in this study is based on the elemental distribution. It means that the amount of each element in input ($W_{i,input}$) should be equal to its amount in the output ($W_{i,output}$).

$$W_{i,input} = W_{i,output} \quad (5)$$

Since an element can exist in different phases, equation 5 can be rewritten as equation 6.

$$W_{i,feed} + W_{i,reducing\ gas} = W_{i,DRI} + W_{i,top\ gas} \quad (6)$$

Where $W_{i,feed}$ is weight of element i in the feed, $W_{i,reducing\ gas}$ is the weight of element i in the reducing gas, $W_{i,DRI}$ is the weight of element i in DRI, and $W_{i,top\ gas}$ is the weight of element i in the top gas.

As it can be seen in Table 1, even in one phase an element can exist in several components. So, equation 6 can be expanded to equation 7.

$$W_{feed} \times \sum_j W_{ij}X_{j\ in\ feed} + W_{reducing\ gas} \times \sum_j W_{ij}X_{j\ in\ reducing\ gas} = W_{DRI} \times \sum_j W_{ij}X_{j\ in\ DRI} + W_{top\ gas} \times \sum_j W_{ij}X_{j\ in\ top\ gas} \quad (7)$$

Where W_{feed} is weight of feed material, $W_{reducing\ gas}$ is weight of reducing gas, W_{DRI} is weight of DRI, $W_{top\ gas}$ is weight of top gas, W_{ij} is weight of element i in component j, $X_{j\ in\ feed}$ is the weight fraction of component j in feed, $X_{j\ in\ reducing\ gas}$ is the weight fraction of component j in reducing gas, $X_{j\ in\ DRI}$ is the weight fraction of component j in DRI, and $X_{j\ in\ top\ gas}$is the weight fraction of component j in top gas.

2.2 Energy balance

The general equation of heat balance can be written as equation 8.

$$\Delta H_{inp} + \Delta H_{out} + \Delta H_{exo} + \Delta H_{end} = 0 \quad (8)$$

Where ΔH_{inp} is enthalpy of input components, ΔH_{out} is enthalpy of output components, ΔH_{exo} is enthalpy of exothermic reactions, and ΔH_{end} is enthalpy of endothermic reactions. The heat of a reaction at temperature T can be calculated by equation 9.

$$(\Delta H_r)_T = (\Delta H_r)_{298} + \sum(H_{298}^T)_{prod} - \sum(H_{298}^T)_{react} \quad (9)$$

Where is $(\Delta H_r)_T$ is enthalpy of reaction at temperature T, $(H_{298}^T)_{prod}$ is enthalpy of product components by changing temperature from 298 K to T, and $(H_{298}^T)_{react}$ is enthalpy of reactant components by changing temperature from 298 K to T. H_{298}^T can be calculated using equation 10.

$$H_{298}^T = n\int_{298}^{T} C_p dT \quad (10)$$

Where n is the mole number, and C_p is heat capacity or the amount of heat energy released or absorbed by a mole of the substance with the change in temperature at a constant pressure. C_p is usually calculated using equation 11(Kubaschewski and Alcock, 1979).

$$C_p = a + bT + cT^{-2} + dT^{-1} \quad (11)$$

Where a, b, c, and d are thermodynamic coefficients which are different for each substance.

2.3 Model assumptions and considerations

Figure 2 shows the schematic flowsheet of the model. As it can be seen, the model consists of two input streams of reducing gas at 900°C and feed material which its temperature should be calculated, and output stream of top gas at 400°C and DRI at 800°C(CHATTERJEE, 2012). In the real process, temperature of shaft furnace can vary from 850°C to 950°C. So, three different temperatures of 850°C, 900°C, and 950°C have been utilized in the model.

Iron ore pellet which is currently used in direct reduction process has been selected as feed material in this study. The chemical composition of the pellet can be found in Table 2.

In the current MIDREX process, the top gas contains approximately 33-37% hydrogen and 21-24% water vapor and CO and CO_2 as the rest, indicating an excess of inlet hydrogen compared to the stoichiometric amount, which is attributed to the process design and considerations(Liu et al., 2014). Consequently, a ratio of 1.7 between hydrogen and water vapor ($H_2/H_2O = 1.7$) has been employed in this model for the top gas. The characteristics of the top gas are detailed in Table 3.

Table 4 illustrates that the reducing gas comprises hydrogen. However, to assess the impact of water vapor on the energy consumption of the process, water vapor was incrementally added up to 10% to the system.

Assuming a 100% metallization degree, the Direct Reduced Iron (DRI) consists of metallic iron and gangue materials, as depicted in Table 5.

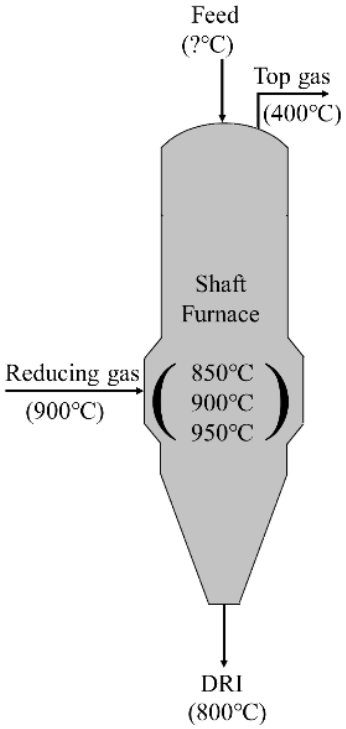

Fig. 2. Schematic flowsheet of model.

Table 2. Chemical composition of pellet (feed material).

Component	Fe_2O_3	Fe_3O_4	SiO_2	CaO	MgO
Mass%	84.64	9.11	3.78	0.73	0.45
	Al_2O_3	TiO_2	MnO		
	0.64	0.23	0.028		

Table 3. Chemical composition of top gas.

Temperature (°C)	400
H_2 (%)	63
H_2O (%)	37

Table 4. Chemical composition of reducing gas.

Temperature (°C)	900
H_2 (%)	90-100
H_2O (%)	0-10

Table 5. Chemical composition of DRI.

Temperature (°C)	800			
Component	Fe	SiO_2	CaO	MgO
Mass%	65.79	3.78	0.73	0.45
	Al_2O_3	TiO_2	MnO	
	0.64	0.23	0.028	

It should be noted that all calculations were carried out for one ton of feed material, and heat loss and mass loss have been neglected. Furthermore, kinetics and rate of reactions have not been considered in the calculations.

3. RESULTS AND DISSCUSIONS

3.1 Thermodynamic studies

Figure 3 illustrates the stability diagram of the Fe-O-H system, known as the Baur–Glässner diagram. Since hydrogen reduction is endothermic, increasing the temperature broadens the stability zone of iron in the diagram. From a thermodynamic perspective, hydrogen reduction should occur at the highest possible temperature, which is also advantageous for kinetics. However, supplying the necessary energy to achieve high temperatures is economically challenging. Furthermore, the diagram shows that in the temperature range of 850-950°C, with up to over 30% water vapor in the system, regardless of kinetics, reduction to metallic iron is still possible. So, in this model 0-10% water vapor considered in the input to be sure that with the produced water vapor from the reduction reactions, it will not exceed from the stable zone of iron.

3.2 Model with preheating feed materials

The heat and mass balance module of the HSC Chemistry software was utilized to model the system when heat is supplied by preheating the feed materials. Figure 4 illustrates the energy required to reduce one ton of pellets using reducing gas with varying water vapor contents. It shows that reduction with pure hydrogen demands 92 kWh at 850°C, 100 kWh at 900°C, and 110 kWh at 950°C. Adding water vapor to the reducing gas consistently decreases the required energy at all temperatures. Figure 5 presents the model results as the preheating temperatures of the feed materials with reducing

gas compositions ranging from 0 to 10% water vapor at operating temperatures of 850°C, 900°C, and 950°C. At a furnace temperature of 850°C with pure hydrogen as the reducing gas, the feed materials must be preheated to 428°C to meet the heat requirements. Raising the operating temperature to 900°C necessitates more energy, requiring the feed materials to be heated to 459°C. Although increasing the furnace temperature from 850°C to 900°C results in a 31°C rise in feed material temperature, raising the furnace temperature to 950°C requires a further increase of 37°C, bringing the feed material temperature to 496°C. This trend persists across different reducing gas compositions.

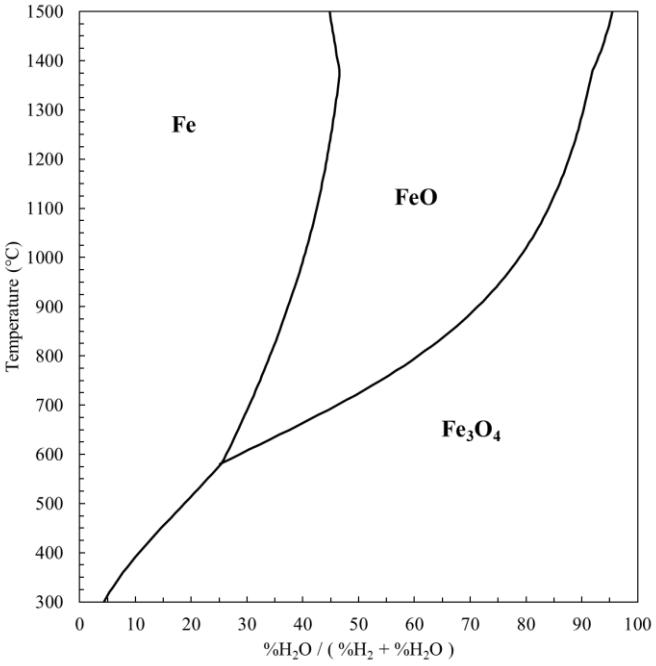

Fig. 3. Baur–Glaessner diagram for Fe-O-H system (calculated with HSC Chemistry version 10.4.1.1).

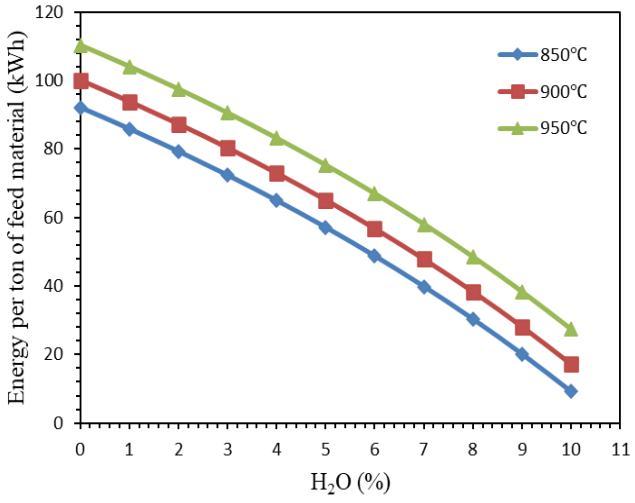

Fig. 4. The required energy to reduce one tone of pellet with different water vapor content in the reducing gas composition.

Figure 5 also shows that at all three operating temperatures, increasing the water vapor content in the reducing gas results in a decrease in the required energy and consequently lowers the preheating temperature of the pellets. To understand this phenomenon, the volume of reducing gas was monitored. Figure 6 displays the volume of reducing gas needed to reduce one ton of pellets with varying water vapor contents. It is evident that increasing the water vapor content raises the volume of reducing gas. Since the top gas composition is maintained at a constant value, as shown in Table 3, increasing water vapor content necessitates an increase in the reducing gas volume to keep the H_2/H_2O ratio constant as per Table 3. Consequently, because the reducing gas is warmer than the pellets, an increase in its volume supplies more heat to the system, significantly reducing the preheating temperature of the feed materials.

Furthermore, Figure 7 illustrates the heat capacity of hydrogen and water vapor at different temperatures ranging from 850°C to 950°C, according to Equation 11. It is observed that the heat capacity of water vapor is higher than that of hydrogen, and for both components, the heat capacity increases with temperature. However, the increase in heat capacity is more pronounced for water vapor than for hydrogen. This indicates that adding water vapor to the reducing gas, even while keeping the gas volume constant, contributes additional energy to the system due to the high heat capacity of water vapor.

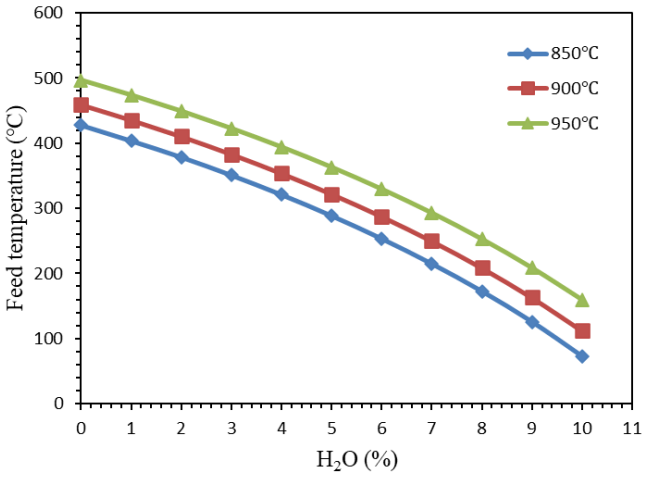

Fig. 5. Temperature of preheated feed materials with different water vapor content in the reducing gas composition.

3.3 Model with oxygen injection

In this model, the necessary heat for the hydrogen reduction process is generated by injecting oxygen into the furnace, facilitated through reaction 4. Figure 8 indicates that to achieve the required reduction heat using pure hydrogen at 850°C, 13.25 Nm³ of oxygen must be injected. When the operating temperature is increased to 900°C, the volume of oxygen needed rises to 14.41 Nm³, and at 950°C, it further increases to 15.87 Nm³. This increase in required oxygen volume with higher temperatures underscores the endothermic nature of the

hydrogen reduction process, which demands more energy input as temperatures rise.

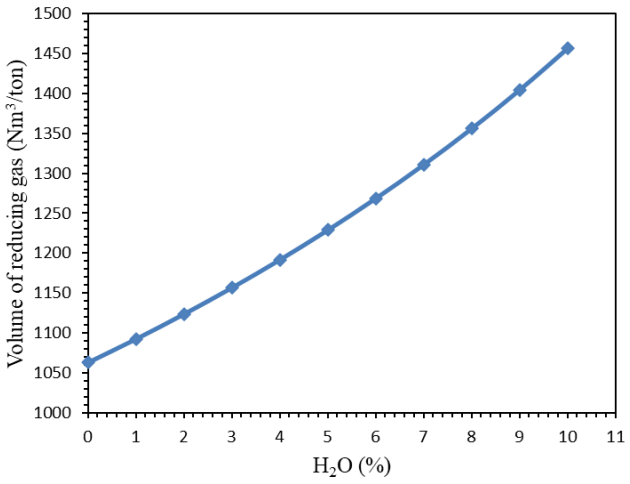

Fig. 6. Volume of reducing gas to reduce one ton of pellet with different water vapor content in the reducing gas composition.

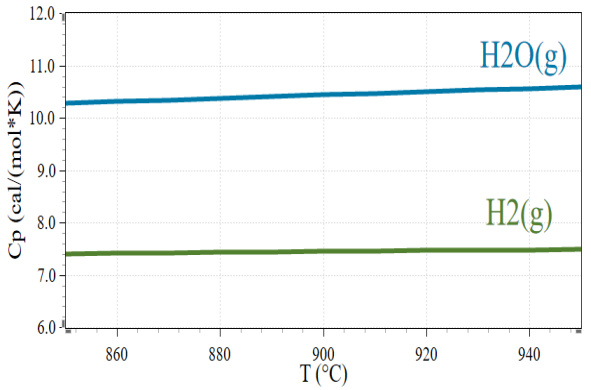

Fig. 7. Heat capacity of hydrogen and water vapor at different temperatures.

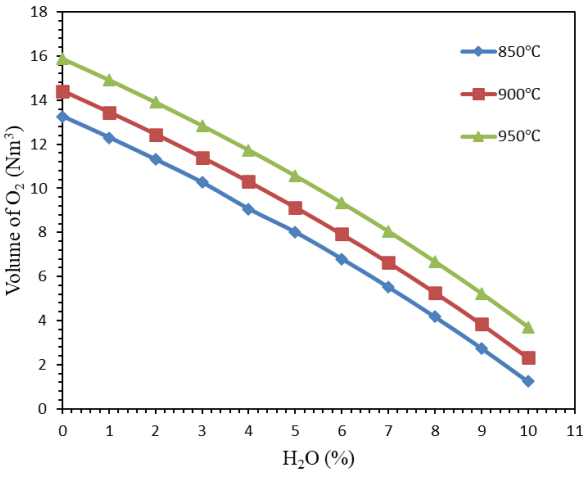

Fig. 8. Volume of injected oxygen with different water vapor content in the reducing gas composition.

Figure 9 illustrates that the volume of reducing gas increases with higher water vapor content, consistent with the earlier discussed principles. However, due to the presence of oxygen in the system, the reducing gas volume also varies with the furnace temperature. As the water vapor content rises, the necessary heat—and consequently the amount of oxygen required—decreases significantly. This reduction in oxygen demand is particularly important because it highlights the interplay between water vapor and oxygen in the system. By optimizing the water vapor content, the process can achieve substantial energy savings and enhanced efficiency.

An ironmaking plant with a capacity of 1 Mt DRI per year can be considered as a realistic example. With the same pellet and gas composition that used in this study, with the reduction temperature of 900°C and 5% H_2O in the system, 65.12 GWh energy is needed for the reduction, which can be supplied by heating the feed material to 322°C or injecting 9.14×10^6 Nm^3 oxygen to the system. Therefore, understanding the precise oxygen requirements at various temperatures and managing both the oxygen injection and water vapor levels are crucial for maintaining an optimal balance of heat supply, reducing overall energy consumption, and improving the economic and environmental performance of the hydrogen reduction process in ironmaking.

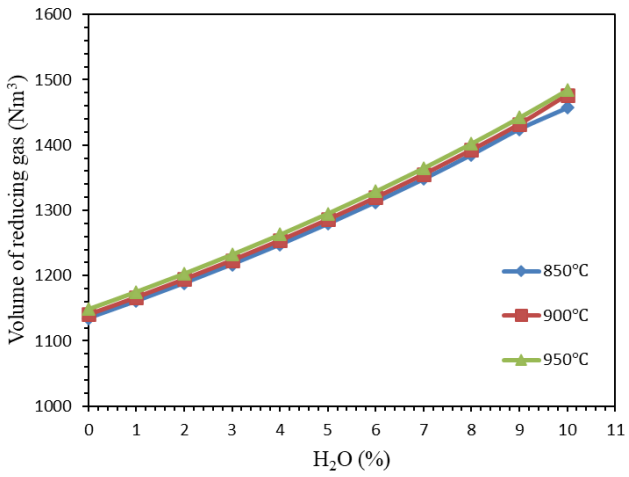

Fig. 9. Volume of reducing gas to reduce one ton of pellet with different water vapor content in the reducing gas composition and the presence of oxygen in the system.

4. CONCLUSIONS

Energy consumption of hydrogen reduction process with the presence of 0 to 10% water vapor was studied in this research. Modeling has been done using the heat and mass module of HSC Chemistry software and with MIDREX condition.

This study offers an in-depth examination of the energy consumption and thermodynamic behavior of hydrogen reduction of iron ore pellets in a shaft furnace. It particularly focuses on the effects of varying water vapor content.

The study reveals that increasing the reduction temperature is thermodynamically favorable for hydrogen reduction, but it necessitates additional energy input, posing economic

challenges. The volume of oxygen required to provide the necessary heat rises with the operating temperature. For instance, 13.25 Nm³ of oxygen is needed at 850°C, 14.41 Nm³ at 900°C, and 15.87 Nm³ at 950°C.

The study also finds that a higher water vapor content augments the volume of reducing gas to keep the top gas composition constant. However, the presence of oxygen in the system also influences the volume of reducing gas to vary with furnace temperature. An increase in water vapor content reduces the heat required and, consequently, the amount of oxygen needed.

By optimizing the water vapor content and operating temperature, the study suggests that significant improvements in energy efficiency and reduction kinetics can be achieved. This enhances the sustainability and cost-effectiveness of the process.

These findings contribute to the development of more efficient and environmentally friendly methods for iron ore reduction in the steelmaking industry. They support efforts to reduce the carbon footprint associated with steel production.

ACKNOWLEDGMENTS

We extend our heartfelt appreciation to the Sustainable Hydrogen - Potential for Bothnia Gulf Cluster project (20357962), funded by the European Regional Development Fund (ERDF), for its invaluable support. We also gratefully acknowledge funding from the Finnish Foundation for Technology Promotion (Tekniikan Edistämissäätiö). The financial contributions from these organizations were instrumental in making this research possible.

REFERENCES

Ahmed, H., Sideris, D., and Björkman, B. (2020). Injection of H2-rich carbonaceous materials into the blast furnace: devolatilization, gasification and combustion characteristics and effect of increased H2–H2O on iron ore pellets reducibility. *Journal of Materials Research and Technology*, 9(6), 16029–16037.

CHATTERJEE, A. (2012). *Sponge Iron Production By Direct Reduction Of Iron Oxide*. PHI Learning.

El-Zoka, A. A., Stephenson, L. T., Kim, S. H., Gault, B., and Raabe, D. (2023). The Fate of Water in Hydrogen-Based Iron Oxide Reduction. *Advanced Science*, 10(24), 1–8.

Fradet, Q., Kurnatowska, M., and Riedel, U. (2023). Thermochemical reduction of iron oxide powders with hydrogen: Review of selected thermal analysis studies. *Thermochimica Acta*, 726, 179552.

Heidari, A., Niknahad, N., Iljana, M., and Fabritius, T. (2021). A review on the kinetics of iron ore reduction by hydrogen. *Materials*, 14(24), 7540.

Kubaschewski, O., and Alcock, C. B. (1979). *Metallurgical Thermochemistry*. Pergamon Press.

Liu, B. N., Li, Q., Zou, Z. S., and Yu, A. B. (2014). Discussion on chemical energy utilisation of reducing gas in reduction shaft furnace. *Ironmaking and Steelmaking*, 41(8), 568–574.

Özgün, Ö., Lu, X., Ma, Y., and Raabe, D. (2023). How much hydrogen is in green steel? *Npj Materials Degradation*, 7(1), 1–5.

Raabe, D., Klug, M. J., Ma, Y., Büyükuslu, Ö., Springer, H., and Souza Filho, I. (2023). *Hydrogen Plasma Reduction of Iron Oxides* (C. Fleuriault, J. D. Steenkamp, D. Gregurek, J. F. White, Q. G. Reynolds, P. J. Mackey, and S. A. C. Hockaday, Eds.; pp. 83–84). Springer Nature Switzerland.

Souza Filho, I. R., Ma, Y., Kulse, M., Ponge, D., Gault, B., Springer, H., and Raabe, D. (2021a). Sustainable steel through hydrogen plasma reduction of iron ore: Process, kinetics, microstructure, chemistry. *Acta Materialia*, 213, 116971.

Souza Filho, I. R., Ma, Y., Raabe, D., and Springer, H. (2023). Fundamentals of Green Steel Production: On the Role of Gas Pressure During Hydrogen Reduction of Iron Ores. *Jom*, 75(7), 2274–2286.

Souza Filho, I. R., Springer, H., Ma, Y., Mahajan, A., da Silva, C. C., Kulse, M., and Raabe, D. (2022). Green steel at its crossroads: Hybrid hydrogen-based reduction of iron ores. *Journal of Cleaner Production*, *340*, 130805.

Spreitzer, D., and Schenk, J. (2019). Reduction of Iron Oxides with Hydrogen—A Review. *Steel Research International*, *90*(10), 1900108.

Sun, M., Pang, K., Barati, M., and Meng, X. (2023). Hydrogen-Based Reduction Technologies in Low-Carbon Sustainable Ironmaking and Steelmaking: A Review. *Journal of Sustainable Metallurgy*, 10, 10-25.